MINIREVIEW

Bimetallic nanocatalysts supported on graphitic carbon nitride for sustainable energy development: the shape-structure–activity relation

Ewelina Kuna, [ID] Dusan Mrdenovic, [ID] Martin Jönsson-Niedziółka, [ID] Piotr Pieta [ID] and Izabela S. Pieta [ID] *

The catalytic performance of metal nanoparticles (NPs), including activity, selectivity, and durability, depends on their shape and structure at the molecular level. Consequently, metal NPs of different size and shape, *e.g.*, nanobelts, nanocubes, nanoflakes, and nanowires, demonstrate different reactivity and provide different reaction rates depending on the facet exposed. In this context, the present review aims to summarize the shape-structure–activity relation of metallic nanocatalysts. Moreover, keeping in mind that the application of noble metal catalysts is expensive, we would like to draw the reader's attention to bimetallic nanocatalysts supported on graphitic carbon nitride. One of the advantages of these systems is the possibility to minimize the use of noble metals by introducing another metal either to the parent NPs and/or modifying the support materials. The development and optimization of bimetallic nanocatalysts might provide the new class of materials with superior, tunable performance, thermal stability and reduced costs compared to presently available commercial catalysts. Therefore, further application of these bimetallic composites for sustainable development in energy, green chemicals/fuels and environmental protection will be discussed.

Introduction

The Paris Agreement, signed by nearly 200 countries at the end of 2015, mandates a significant reduction in carbon emissions worldwide, which will require major changes in the way the world produces and uses energy.[1] Meantime, a 50% increase in global energy demand is predicted by 2035, resulting in an urgent need for new technologies that will form the backbone of the future energy system.[2] Besides carrying economic and social benefits, these new technologies have to be sustainable and adaptable to the change of climatic conditions. By developing novel chemical conversion routes and novel fuels, catalysis science can make an important contribution to solving this conundrum through the diversification of renewable fuels or the production of green chemicals.[3] Therefore, clean energy and fuels, as well as green chemicals synthesis, are critical for our future and are of the highest impact in today's research.[4] This sustainable development can take the form of harvesting solar energy, conversion of biomass to biofuels or chemicals, and pollution control as examples of up front to downstream solutions.[5] In certain cases, the industrial processing is run in homogenous phase reactors.[6] However, for ease of separation and often for lowering the environmental impact, a transition to heterogeneous phases and catalysis usage is often preferred. In

some of these processes, noble and transition metal-based catalysts are used, *e.g.*, Pt, Pd or Ni, due to their high inherent reactivity. These transition metals have been attracting considerable attention regarding to their enhanced activity, stability and/or selectivity in various reactions such as reforming,[7–9] decomposition,[10] partial oxidation,[11–17] hydrogenation,[18,19] *etc*. Unfortunately, despite their promising physical properties, their activity and selectivity for processes still require further understanding. Furthermore, noble metal catalysts are expensive, usually making the process economically infeasible. Thus, improving heterogeneous catalytic performance (the activity, selectivity, and durability) and minimizing the use of noble metals are remaining challenges in numerous significant reactions. For the same reason, noble metal catalysts synthesis protocols need to be developed along with a suitable support to possibly induce a synergetic effect between all components correlated with catalytic performance.[20] Recently, the authors point to the shape and size dependency of the catalyst performance for various reactions over monometallic nanoparticles (NPs) and well-defined clusters, especially noble metals.[21,22] They exhibit unique size-dependent physical and chemical features, including optical, magnetic, catalytic, thermodynamic, and electrochemical properties. Some studies show a decrease in catalytic activity as the particle size is decreased to an optimized nanoparticle dimension, *e.g.*, for the CO oxidation on Pt, Pd or Au NPs.[11] Other catalytic reactions showed enhanced catalytic

Institute of Physical Chemistry Polish Academy of Sciences, 01-224, Warsaw, Poland. E-mail: ipieta@ichf.edu.pl

performance with the increase of NPs size in a given range, usually due to the fact that smaller particles provide a very strong reactant or product molecules binding which suppresses a coupling with another species on a catalyst surface, *e.g.*, the CO oxidation on a supported Pt/Al$_2$O$_3$ catalyst.[8,11,23] Most of those size-shape dependency studies are performed for monometallic systems and well defined clusters, especially for noble metals.[24] In contrary, bimetallic and multicomponent NPs and their catalytic activity have been reported in literature, however, there are few studies addressing size and/or shape-dependency of their catalytic performance.[7,22,23]

In the present review we intend to provide our readers with more information about bimetallic catalytic systems. In particular, we would like to point to the structure–property relationships at the molecular level (including metal–metal and metal–support interactions). The integration of *in situ* studies with a fundamental understanding of size and shape-dependent catalytic performance is therefore significant as it allows for authentic and accurate consideration of size- and shape-dependent catalytic activity.[25,26] Finally, using some representative examples of the graphitic carbon nitride supported bimetallic NPs systems, further potential applications of these catalysts will be demonstrated. A better understanding of the bimetallic catalytic system will provide the opportunity to develop new green synthesis protocols for the chemical, clean energy, new technology and pharmaceutical industries, where high efficiency and selectivity play a pivotal role.

The shape-structure–activity relation of bimetallic catalysts

Synthesis and characterization of a bimetallic catalytic system

Alloying a parent metal with a second metal offers numerous opportunities to tune the electronic states of the catalysts and optimize their catalytic properties.[21] Not surprisingly, bimetallic nanoparticles (NPs) have gained popularity, as compared to monometallic NPs, evidencing better catalytic features.[21,22,25–27] Bimetallic NPs can be synthesized with various morphologies and geometries, depending on the preparation method, temperature, and atmosphere of pre-treatment used (Fig. 1).[24,30] One of the advantages of bimetallic catalysts is the possibility of performance tuning through the varying structure by introducing another metal to the parent nanoparticle.[31,32] The synthesis of these advanced nanomaterials has been facilitated by technology development that have enabled their preparation with tunable compositions, shapes, sizes, and structures, either on their own or on support materials.[33] The synthesis protocols of various types of bimetallic NPs and their composites have already been addressed by many researchers and reported in literature.[34]

The bimetallic particles' structure can be tailor-designed by synthesis protocol or randomly attained, *i.e.*, intermetallic compound, alloy, core–shell or clusters structures, *etc.*[35] In fact, their final structure strongly depends on several parameters such as (i) composition, (ii) synthesis methodology applied and conditions, (iii) relative strengths of the metal–metal bond,
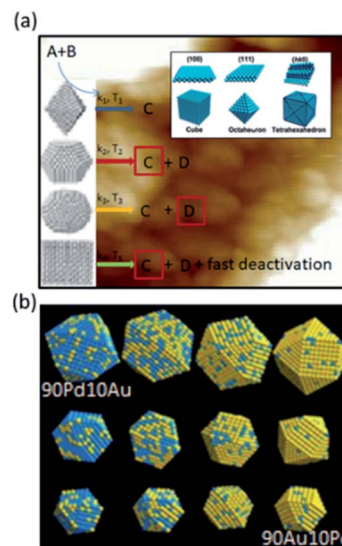

Fig. 1 (a) The shape–activity relationship at molecular level. (b) The example of Au–Pd nanoparticles for different Pd : Au concentrations. This figure has been adapted from ref. [21] with permission from Royal Society of Chemistry, copyright 1972; and from ref. [24] with permission from American Chemical Society, copyright 2007.

surface energies of bulk elements, and many more as given previously.[36,37]

Considering several essential processes, such as hydrogenation, dehydrogenation, and isomerization and a variety of bimetallic catalysts applied for them (*i.e.*, Ni–Cr, Ru–Cu, Os–Cu, Pt–Ir, Pt–Ru), there is an undoubted correlation between shape yet also between the shape and chemical composition of selected bimetallic nanostructures towards given functionality. Moreover, by varying ratios of both metals, the selectivity of the reaction, as well as the product distribution, can be controlled, *i.e.*, as was shown for Ru–Cu catalyst for glycerol hydrogenolysis.[38] Also, material composition with tuneable interparticle distance affects the catalyst's stability in a chemical reaction. The inclusion of additional metal in bimetallic nanostructures influences (i) the NPs size and overall bimetallic nanocatalysts lifetime; (ii) changes the electronic configuration thereby creates ligand and strain effects.[39,40] These aspects still require basic research and essential consideration to improve the charge transfer phenomena, altering the binding energy, and reducing the obstacles for specific chemical reactions, providing a shield from catalyst poisoning and catalytic deactivation. Moreover, the NPs tuneable composition can enhance the thermal stability of bimetallic NPs in certain chemical reactions and gives a possibility to reduce the poisoning effect creating a new reaction pathway leading to a distinct product distribution with the desired selectivity.[41,42]

Apart from synthesis, another crucial aspect is understanding how a heterogeneous catalytic system works, and most importantly, how it works under 'not isolated' conditions. To address this issue, the selected catalytic process is often broken down into simplified steps and chemical reactions that adequately simulate the catalytic material and/or conditions,

focusing each time on an isolated part of the catalytic process.[28,29,43] Therefore, the chemistry and structure of many bimetallic catalysts should be studied under reaction conditions or ducting catalysis by *in situ*/operando techniques. Such studies allow to establish an intrinsic correlation between the chemistry and the structure of the authentic surface catalysing a reaction and the corresponding catalytic performance. Furthermore, valuable inputs on the atomic (*i.e.*, microscopic) level, catalyst surface and intermolecular interaction are obtained from surface science and theoretical chemistry, which are further used as a basis for understanding the complex structures and catalytic behaviour of real materials under operating conditions.

Morphology and activity of bimetallic NPs

Structural arrangement and coordination environment of atoms in the catalytic system provide different active sites, which further influence the adsorption energy of reaction intermediates, the activation energy of their transition states and the bond-breaking mechanism of these chemical species on the catalyst surface.[44–46] In the bimetallic system, the incorporation of second metal changes the bond lengths between metals and hence influences the geometric and electronic structure of catalyst.[44,46] Thus, bimetallic NPs with distinctive morphology possess different catalytic activity. In the literature, most of the size-shape dependency studies are performed for monometallic systems and well-defined clusters, especially noble metals. Unfortunately, only a few research groups have practical experience in the bimetallic, noble metal-free NPs synthesis and studying structure–activity correlations.[7,21,22] Therefore, these sparse data available in the literature are discussed below with respect to the shape–activity relationship studies on bimetallic catalytic systems.

The NPs activity as well as NPs morphology depends on the NPs surface properties, whereas the surface structure depends on the size and shape of NPs. Metallic NPs with diverse shapes profiles (*i.e.,* nanobelts, nanocubes, nanoflakes, nanowires) may have different exposed facets. The exposed crystal facets are differing in atomic and electronic structures and hence possess various catalytic properties. Therefore, the exposure of different crystal facets can significantly change catalytic activity for a given chemical reaction.[46] For instance, it has been found that monometallic Pt nanocrystals terminated with high-index (730) facets exhibited an excellent activity for electrooxidation of ethanol and formic acid.[46,47] However, in the bimetallic system, the catalytic activity may follow a completely different order for various exposed facets than its monometallic counterparts. This has been demonstrated by studies on oxygen reduction (ORR) activity on the Pt surface. As noticed, for bare Pt surface, the ORR activity increases in the order of Pt (100) < Pt (110) < Pt (110). Whereas, for Pt$_3$Ni alloy, the ORR activity increases in the order of Pt$_3$Ni (100) < Pt$_3$Ni (110) < Pt$_3$Ni (111).[46,48] Furthermore, it was found that lattice strain might strongly affect the catalytic activity of NPs. For example, icosahedral and octahedral Pt$_3$Ni nanocrystals both terminated with (111) facets reveal different ORR activity.[48] The higher percentage of edge atoms in
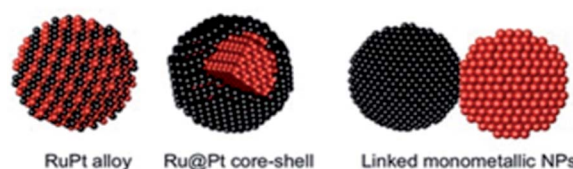

Fig. 2 Different types of Ru–Pt bimetallic system. This figure has been adapted from ref. [51] with permission from Springer Nature, copyright 2008.

icosahedral Pt$_3$Ni results in the higher mass and area-specific activity, changing the adsorption energy and hence boosts catalytic performance.[46,48]

Typically, depending on the synthesis and temperature used, three types of architectures/structures can be distinguished in bimetallic catalytic systems, *i.e.*, alloys, core–shell, and contact aggregates (Fig. 2).[48–51] For these catalytic systems, the metals' atomic distribution is another crucial factor that may affect the catalytic activity. The atomic distribution in core–shell and alloy structures can be adjusted by the different ratio of the two metals or by the degree of alloying. As reported by Choi *et al.,* for Pt$_x$Co alloy the highest ORR activity was obtained for Pt$_3$Co nanocubes.[46,49] It was found that the catalytic activity corresponds to the different oxygen-binding energy of various Pt to Co ratios. On the other hand, in some cases, the catalytic activity of bimetallic Au–Pd alloys and Au@Pd core-shells which possess the same atomic distribution can be different.[46,50] Therefore, to estimate the catalytic activity, it is important to predict the structure of the NPs catalytic system. The architecture of metallic NPs can be estimated by the binary phase diagram of the bulk alloy and its corresponding thermodynamic model.[52] The shape-temperature dependency for Cu–Ni NPs showed that the Cu–Ni alloy can only be synthesized at temperatures higher than that at which the two metals mix together (miscibility temperature, (mT)).[52] If the temperature is below the mT, the alloy cannot form and a "Janus" NP is created instead (Fig. 3). This first theoretical study can support the experimentalists by guiding them in their attempts to synthesize bimetallic NPs with the desired structure and, hence, catalytic activity.[52] Indeed, it was confirmed that different Pt–Ru NP catalyst architectures provide different activities in the preferential oxidation of CO in H$_2$ (Fig. 4).[51,53] Importantly, different catalytic activity is also observed for bimetallic NPs, which possesses different particle size, *e.g.*, in the case of the CO oxidation on Pt, Pd or Au nanoparticles.[54,55] As noticed, the catalytic activity decreases as the particle size decreases until
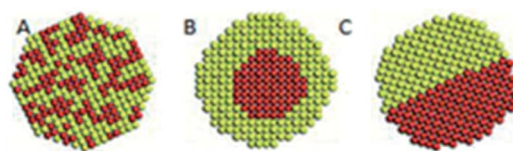

Fig. 3 Cu–Ni nanoalloy (A) mixed, (B) core–shell, (C) Janus nanoparticle. This figure has been reproduced from ref. [52] with permission from The Royal Society of Chemistry, copyright 2009.
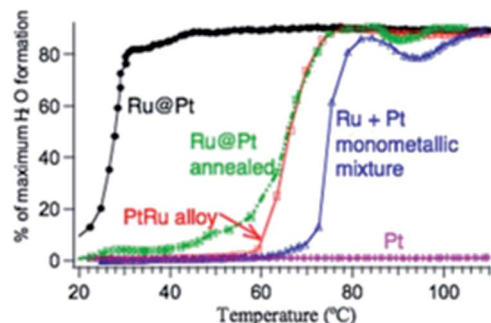
Fig. 4 Activity of different Pt–Ru bimetallic systems in preferential oxidation of CO in H_2. This figure has been adapted from ref. [51] with permission from Springer Nature, copyright 2008.

the optimized nanoparticle size is achieved. However, it has been found that some catalytic reactions show an increase in catalytic performance with an increase in the catalyst nanoparticle size (within a given range). This phenomenon was observed mainly for the CO oxidation on supported Pt/Al_2O_3 and for the Fischer–Tropsch reaction performed on Co-bases catalyst.[56] The decrease in the catalytic activity can be explained by the fact that smaller particles bind the reactant or product molecules more strongly, which suppresses coupling with another.

For the bimetallic system, the change of particle size is mainly related to the change of atomic-scale structure.[45] With the decrease of NPs size, two metals' distribution differs spontaneously to minimize the surface energy and form the most thermodynamically stable mixing pattern.[45] For instance, the optimal NPs size of Pt–Co alloyed catalysts, designed for chemical energy conversion into electricity in fuel cell was studied *via in situ* atomic-level imaging.[57] Applied measurement method revealed the structural and compositional changes at the atomic level during the thermal treatment (annealing process) of NPs and allowed for the best catalytic performance correlation with the optimal structure (Fig. 5).[58] This study clearly demonstrated the need for *in situ/operando* characterization in order to tune the material for a given functionality.

The complexity of the surface structure

The structure of bimetallic system not only has a significant influence on the catalytic properties but also can undergo
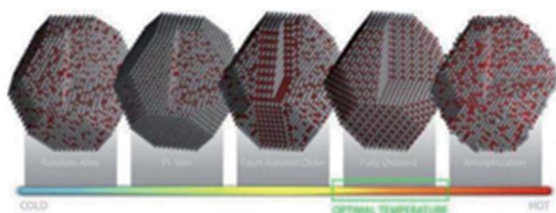

Fig. 5 Co atoms on graphene – behaviour at the atomic scale when alloying nanoparticles during *in situ* annealing. This figure has been reproduced from ref. [58] and [59] with permission from Springer Nature, copyright 2015.

constant changes under reaction conditions due to the atomic reorganization.[45] Therefore, the NPs surface properties have to be taken into account when selecting the suitable catalytic system. For bimetallic NPs catalyst, both surface topography (*i.e.*, NPs distribution on the investigated support) and surface chemistry (*i.e.*, composition of the system different than the composition of the bulk) should be considered. In principle, in terms of topography, the surface reconstruction and surface energy minimization lead to the NPs arrangements. Whereas, from the chemical point of view, the component segregation enriches surface layers into one component compared to the bulk composition. Therefore, both topography and surface chemistry have a crucial impact on the catalytic activity.

XPS studies of the CO oxidation on Rh indicated that the higher turnover rates are due to the oxidation state of Rh change from metallic rhodium to Rh^{3+}.[59] Similar studies carried out on Pt and/or Pt–Rh NPs, also confirmed that oxidation state has a direct influence on the final reaction rate. Obtained results pointed out that the NPs size is in direct relation to the oxidative state of NPs (*e.g.*, Pt NPs below 1.5 nm are in the 2^+ and 4^+ oxidation state).[55] This might be explained by the fact that very few bulk atoms are available for these nanoparticles. Therefore, they are dominated by low-coordination surface atoms, and, as a result, their electronic structure changes. In a model example, different surface geometrical arrangements are formed over a single crystal surface, depending on the direction in which they were grown. The NPs direction grown ultimately determines the frequency with which the chemical reaction undergoes cyclic oscillations, as in the case of Rh surfaces exposed to oxygen and hydrogen.[29] In other words, the surface geometric arrangement influences the different adsorption affinity of the selected substrate and thus overall catalytic activity.

Another crucial aspect, in the context of surface complexity, is the phenomenon known as strong metal-support interaction (SMSI).[60] The SMSI describes a strong oxide support effect on catalytic reaction rates, where the oxide itself does not perform the same or any chemical reaction. Tailoring multiple catalytic active sites, especially acidic and basic sites on solid supports, provides opportunities for the development of new green synthesis protocols for the organic synthesis and chemical industry. The SMSI effect will be described in the following chapters using the graphitic carbon nitride supported bimetallic NPs as an example.

Bimetallic NPs supported on carbon nitride

Properties of graphitic carbon nitride

Graphitic carbon nitride (g-C_3N_4) is a polymeric material predominantly composed of carbon and nitrogen.[61] Therefore, the g-C_3N_4 consists of the three triazine subunits merged in a planar triangular arrangement (called tri-s-triazine ($C_6N^7H_3$)).[62–65] As shown in Fig. 6a, the tri-s-tirazine is an aromatic ring connected through the planar tertiary aminogroups in a layer, forming a stacked 2D structure. The 2D
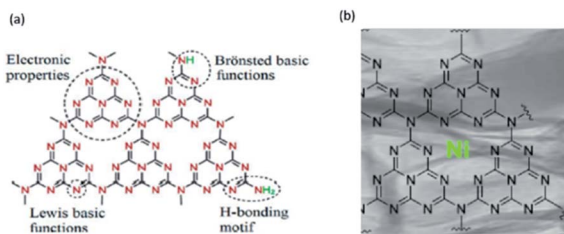
Fig. 6 Scheme of (a) pure and (b) doped graphitic carbon nitride (g-C_3N_4) structure and its properties. This figure has been adapted from ref. [63] with permission from American Chemical Society, copyright 2009; and from ref. [64] with permission from Elsevier, copyright 2019.

structure of tri-*s*-tirazine can be regarded as an *N*-substituted graphite framework (with the highest nitrogen-doping level) consisting of π-conjugated graphitic planes, which are formed *via* sp^2 hybridization of carbon and nitrogen atoms.[62]

g-C_3N_4 can be synthesized *via* a one-step polymerization of cyanamide, urea, thiourea, melamine, or dicyandiamide. The high degree of polycondensation reaction leads to high thermal stability (up to 600 °C) and to good chemical resistance.[65] Various strategies of the synthesis, templating and post-processing of carbon nitride provide the possibility to adjust optical, electronic, and physicochemical properties.[66] Whereas the low cost of the starting materials and the easy of preparation open a wide range of applications in energy storage and conversion, especially in the field of photo-, electro- and thermal catalysis.

Furthermore, g-C_3N_4 has rich surface properties that are important for catalysis, such as basic surface functionalities, electron-rich properties, and H-bonding motifs (Fig. 6b). Therefore, pristine g-C_3N_4 has been reported as a promising catalyst for various reactions, including CO_2 activation,[67] transesterification,[68] oxygen reduction,[69] hydrogen production[70] or photodegradation of dyes, *etc*. Importantly, the functional groups on the g-C_3N_4 surface make it an ideal support candidate for dispersed small metallic NPs, showing a strong affinity for them, and preventing their agglomeration.

Potential application of NPs/g-C_3N_4 system in thermal catalysis

g-C_3N_4 possesses unique surface properties that might affect its further application towards standard (thermal) catalytic processes. Nitrogen functional groups at the surface can act as strong Lewis base centres. Therefore, both unmodified and modified g-C_3N_4 (doped metal systems) can be directly employed as an effective catalyst for the oxidation reaction of cyclic olefins, alcohols, toluene and benzene.[71]

Furthermore, the NPs/g-C_3N_4 catalysts can be applied in C–C bond formation *via* alkene/alkane dimerization.[72] As an example, the graphitic carbon nitride based catalysts were active for Knoevenagel condensation, *i.e.*, the reaction between an aldehyde and an active methylene-containing reagent.[73] This reaction is a primary path to synthesize valuable β-unsaturated carbonyl compounds that are widely used in the pharmaceutical industry. It is worth mentioning here that the presence of

metallic alloy particles implies a likely activity as catalysts for "redox" reactions, such as oxidation and hydrogenation/dehydrogenation reaction. Whereas the graphitic carbon nitride supports exhibit a basic catalytic behaviour and, in contrast to commonly applied support oxides, poor reactivity towards metals.[74] Thus, the NPs/g-C_3N_4 catalyst might be much more stable catalyst in comparison to their commercial counterparts. Therefore, coupling the acido-basic properties of the nitride carbon support and the properties of the metallic alloy particles, gives a possibility to perform complex reactions (such as hydrocondensations or dehydrocondensations), providing attractive routes to fuels and chemicals.

Finally, the polar C–N–C groups of g-C_3N_4 can provide ideal adsorption sites for polar molecules. *e.g.*, NO, N_2O, facilitating the molecules reactivity and product desorption. This feature and strong resistance to oxygen make g-C_3N_4 a suitable catalyst support for the oxygenated pollutants decomposition, *e.g.*, challenging N_2O decomposition reaction.[75,76] In recent years, many catalysts have been studied and Ru NPs were considered as having one of the best activities among the metals (an effective N–O bond dissociation catalyst), depending on the size and support. Nevertheless, *in situ* DRIFTS studies confirmed that in general the N_2O adsorption and its decomposition lead to oxygen species that are not easily desorbed from metallic Ru NPs. Thus, once formed oxygen species caused the formation of a high valence state of Ru (Ru^{4+}) and further deactivation of catalyst.[77] Therefore, the design and development of new and active NPs/g-C_3N_4 catalysts, which can contribute to the greenhouse gas reduction and sustainable energy development, is still required.

Photo- and electrocatalytic application of bimetallic NPs/g-C_3N_4

g-C_3N_4 is considered as a kind of multifunctional catalyst.[78] Nevertheless, due to its unique electronic band structure, this semiconductor material has found application mainly in the photocatalytic field. The van der Waals interactions between adjacent C–N layers with strong covalent bonding within each layer are involved, implying its stability under light irradiation in solution.[79] However, g-C_3N_4 with a medium band gap energy (2.7 eV) suffers from the rapid recombination of photogenerated electron–hole pairs, inefficient visible light utilization, and a small specific surface area.[64,80,81] All above-mentioned factors suppress its photocatalytic activity. Therefore, to overcome these limitations, the g-C_3N_4 structure can be modified. Modification strategies, starting from various synthetic methods of pristine g-C_3N_4 and ending with the combination of g-C_3N_4 with other nanomaterials, such as metals, oxides, metal oxides, metal sulfides or halides. There are several reports describing the fabrication of g-C_3N_4-based nanocomposites and the underlying mechanisms of their photocatalytic performance.[78,81] Nevertheless, the complex mechanistic studies on the bimetallic NPs/g-C_3N_4 system are rather barely reported in the literature.

The photocatalytic activity of metallic systems based on g-C_3N_4 depends mainly on the metal–semiconductor junction
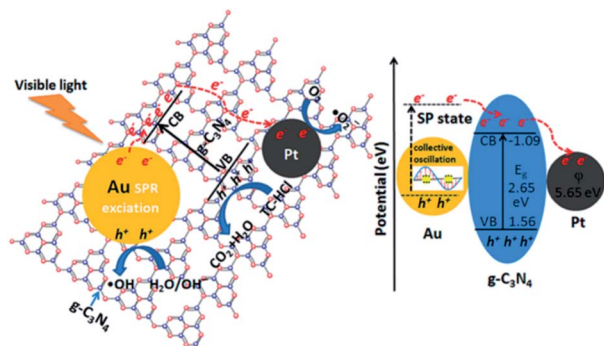
Fig. 7 Proposed photocatalytic mechanisms for the degradation of tetracycline hydrochloride (TC-HCl) by Au@Pt/g-C$_3$N$_4$ nano-composites under visible-light irradiation. SP-surface plasmon. This figure has been adapted from ref. [91] with permission from American Chemical Society, copyright 2015.

(called the Schottky junction) and the surface plasmon resonance (SPR) effect, rising from noble metal NPs.[81] The creation of heterojunctions in g-C$_3$N$_4$ semiconductor structure allows for the formation of a tuneable space-charge separation region. Therefore, once modified semiconductor can more effectively capture photogenerated electrons and reduce recombination of photogenerated carriers. Consequently, the prolonged lifetime of electron–hole pairs increases the overall catalytic performance. Furthermore, incorporation of any noble metal into semiconductor structure might cause the SPR effect. The SPR effect can result in a significant local electric field enhancement (at the surface of NPs), interacting with the conduction band of the contacted semiconductors and, hence, increasing its (photo)reactivity (Fig. 7).[82,83] For the same reason, noble metals are regarded as an appealing co-catalyst in the construction of heterojunctions for photocatalytic applications.

The bimetallic NPs/g-C$_3$N$_4$ materials can catalyse chemical transformations, that are not achievable for its monometallic counterparts, owning to the specific functions in the overall reaction mechanism.[84,85] The addition of a second metal in the catalytic system has a huge impact on the activity, selectivity, and, in some cases, non-toxicity of photoactive composites.[81,86] Not surprisingly, the bimetallic NPs/g-C$_3$N$_4$ systems have been successfully applied in the pollutant degradation,[87] hydrogen evolution[88,89] or CO$_2$ reduction.[90] As an example, an increase in the photocatalytic activity of Au–Pt/g-C$_3$N$_4$ was observed for the organic pollutant degradation, i.e., tetracycline hydrochloride (TCH-Cl), (Fig. 7).[90] In comparison to Pt/g-C$_3$N$_4$ and Au/g-C$_3$N$_4$, the conversion rate for the bimetallic system increased from 67% and 79% up to 93%, respectively. A similar trend can be observed as regards to the hydrogen evolution reaction for the gold-palladium bimetallic system. The Au–Pd/g-C$_3$N$_4$ provides high hydrogen evolution efficiency, which is 1.6 and 3.5 times higher than those of Pd/g-C$_3$N$_4$ and Au/g-C$_3$N$_4$.[80,92]

The synergetic metal effect is also crucial in the development of an efficient catalyst for the CO$_2$ reduction. The carbon oxide reduction (CO$_2$RR) is a challenge for artificial photosynthesis, mainly due to short-term stability of photoactive materials and their low selectivity towards CO production.[93] Nevertheless,

CO$_2$RR can be performed applying electrocatalytic processes. Recent studies show that the bimetallic NPs/g-C$_3$N$_4$ can significantly improve the CO$_2$ reduction performance.[91,94] The Ni–Mn/g-C$_3$N$_4$ and Ni–Cu/g-C$_3$N$_4$ catalysts are found to be more efficient than their monometallic counterparts.[90] For these systems, CO evolution, reached approx. 90% over a wide potential range (−0.6 V to −0.9 V vs. RHE electrode) with a low overpotential of 0.39 V vs. RHE. It is supposed that the enhanced activity coming from the synergetic effects of two metal species and the atomically dispersed unsaturated coordination between metal and the g-C$_3$N$_4$ matrix. If g-C$_3$N$_4$ is hybridized/doped/modified with a conducting material, also in the nanostructure form, then it may be possible to obtain a stable and active material (i.e., as anode for electrochemical reaction), as a result of the individual components. In this context, g-C$_3$N$_4$ may stabilize the NPs arrangement, while transition metal/metal alloys strongly enhance the electrocatalytic activity, improving the performance due to the adsorption capacity.[95–98]

Therefore, the bimetallic NPs/g-C$_3$N$_4$ system can be applied towards other electrochemical reaction such as electrooxidation of alcohols, e.g., methanol, ethanol, ethylene glycol and glycerol. In general, the electrooxidation of these small organic molecules takes place at the Pt-based anodes and is limited by several inherent drawbacks, including high cost and high susceptibility to CO and HCO poisoning.[99] The performance of Pt electrodes is also inadequate for practical applications because of the slow kinetics of the methanol oxidation reaction (MOR) and the oxygen reduction reaction (ORR) compared to current noble metal catalysts.[100–104] To overcome these problems, high-efficient but low-cost anode catalysts was developed. Catalysts that are not based on precious metals, such as Pt or Pd, but various graphene derivatives or carbon nanotubes. Indeed, it was found that, e.g., bimetallic Pt–Pd/g-C$_3$N$_4$-CB (see Fig. 8) showed excellent catalytic activity and durability for electrooxidation of alcohols in alkaline media.[101] On the other hand, platinum metal catalysts combined with transition metals, like Fe, Co, Cu or Ni, exhibited high performance in many reactions and could achieve higher ORR activity.[98–103]

An interesting alternative for the electrocatalytic oxidation reaction is the combination of photo- and electrochemistry.[103] The Cu–Ni bimetallic NPs embedded carbon nitride can be used as electrocatalysts with high MOR efficiency, stability, and
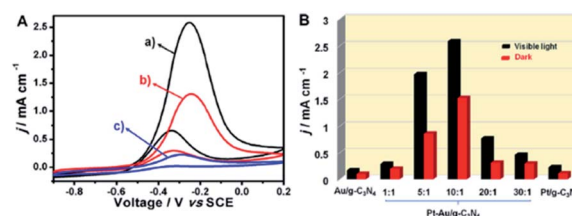

Fig. 8 (A) Cyclic voltammogram of Pt–Au (10 : 1)/g-C$_3$N$_4$ (a and b) and Pt/g-C$_3$N$_4$ (c) electrodes under visible-light illumination (a) and under dark (b and c), respectively. (B) The histogram of activities of different electrodes with different ratio of Pt and Au for MOR upon visible light and dark environment. This figure has been adapted from ref. [104] with permission from Elsevier, copyright 2020.
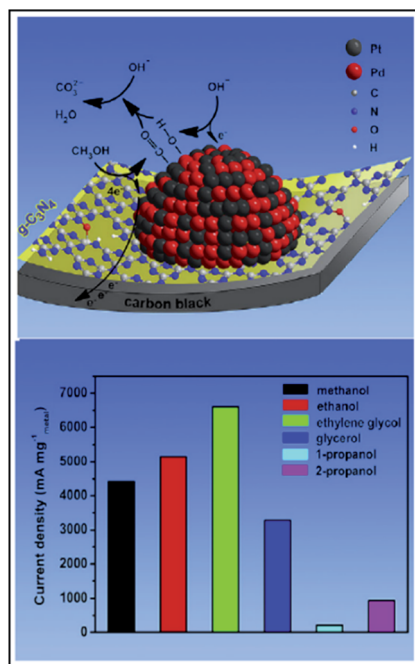
Fig. 9 The mechanism of enhanced catalytic activity of Pt–Pd/g-C_3N_4-CB for alcohols electrooxidation. This figure has been adapted from ref. [102] with permission from Elsevier, copyright 2020.

performance for the electrooxidation of methanol.[64] Similar results were obtained for Pt–Au/g-C_3N_4 composites. Comparing with Pt/g-C_3N_4 modified electrode, Pt–Au/CN exhibited 13.8 times enhancement on the electrocatalytic activity of MOR (Fig. 8).[64,104]

From the point of biofuel electrochemical transformation, this bimetallic catalyst is of substantial importance in enabling fuel cell technology. Furthermore, the performed study pointed out that the tuneable transition metal stoichiometry and the surface chemical composition and morphology optimization can be adapted for current density and photocurrent regulation (Fig. 9).[64,102,103]

Conclusions and outlook

This review has endeavoured to highlight the exceptional versatility of graphitic carbon nitride supported bimetallic nanocatalysts for sustainable energy development. The bimetallic NPs catalysts systems are already known in the literature. As mentioned, bimetallic NPs can be synthesised following a various synthetic methodology which allows controlling their structure, composition, size, and morphology. All these parameters influence the geometric and electronic structure of the catalyst and hence its catalytic activity. The structural arrangement and coordination environment of atoms in bimetallic system determine the adsorption and activation energy. Depending on it, some bimetallic catalysts may then favour given chemical reaction. Nevertheless, it still is difficult to predict how exactly individual parameters, e.g., size of NPs or composition of the bimetallic system, can provide the best catalytic performance for the selected chemical reaction. The diversity of catalyst morphologies and geometries provides

different accessibility to active sites, which can differ from single nanocrystal to bulk metal surface, and change upon reaction conditions e.g., via surface segregation. Therefore, fundamental studies, at the molecular level, of how the shape and structure of bimetallic NPs affect their catalytic activity are still required also during the application process. A comprehensive study on the structure–property correlation relating to the atomic-level can be achieved by the in situ microscopic technique. Moreover, a better understanding of the shape-structure–activity relation at the metal–metal and metal-support level allows the design of a new class of more eco-friendly materials in which the use of expensive noble metal can be decreased.

Special attention should be raised on the supporting material and its further interaction with metallic NPs. Herein, graphitic carbon nitride (g-C_3N_4) has been considered as one of the most promising supporting material due to its unique physicochemical properties. As mentioned, g-C_3N_4 can be applied towards thermo-, photo-, and electro-catalysis. Therefore, the possibility of combining metal NPs with g-C_3N_4 opens a new class of bimetallic nanocatalysts that can find an application in clean chemical synthesis and clean energy production. Importantly, the design of these complex materials should begin with the rational synthesis of individual components, i.e., bare g-C_3N_4 and bimetallic NPs, and end up with their suitable functionalization. This allows to tune the electronic structure of the supporting material, e.g., optimize the light absorption, the charge carrier separation/transportation, and improve its surface properties, e.g., increase the g-C_3N_4 Lewis active sites. Therefore, the use of g-C_3N_4 exerts the stability of bimetallic NPs, e.g., inhibits the poisoning of NPs catalyst, and, thus, enhances the overall catalytic performance.

It has been proved that the bimetallic NPs/g-C_3N_4 system exhibit higher catalytic activity in comparison to their mono-metallic counterparts in several chemical reaction, such as hydrogen evolution, CO evolution or electrochemical oxidation of small organic molecules. Although considerable progress has been achieved, further studies can be devoted towards the N_2O decomposition, CO_2 hydrogenation and/or C–C formation. In particular, additional in situ studies on the reaction mechanism/reaction kinetics are required. These studies can contribute to energy-related global issues by the development of a new catalysts, with superior, tuneable performance, thermal stability, and reduced costs.

Conflicts of interest

There are no conflicts to declare.

Acknowledgements

Notes and references

1 https://treaties.un.org/doc/Publication/CN/2016/CN.735.2016-Eng.pdf.

2 https://www.circleofblue.org/2011/world/eia-worlds-energy-use-to-double-by-2035-driven-by-fossil-fuels-in-china-and-india/.

3 D. L. Klass, *Biomass for Renewable Energy, Fuels, and Chemicals Book*, Entech International, Inc., The Netherlands, 1998.

4 D. Parlevliet and N. R. Moheimani, *Aquat. Biosyst.*, 2014, **10**, 4.

5 F. Tonelli, S. Evans and P. Taticchi, *Int. J. Bus. Innovat. Res.*, 2013, **7**, 143.

6 C. M. Friend and B. Xu, *Acc. Chem. Res.*, 2017, **50**, 517.

7 S. Arora and R. Prasad, *RSC Adv.*, 2016, **6**, 108668.

8 M. García-Diéguez, I. S. Pieta, M. C. Herrera, M. A. Larrubia and L. J. Alemany, *J. Catal.*, 2010, **270**, 136.

9 M. García-Diéguez, I. S. Pieta, M. C. Herrera, M. A. Larrubia and L. J. Alemany, *Appl. Catal., A*, 2010, **377**, 191.

10 G. Centi, A. Galli, B. Montanari, S. Perathoner and A. Vaccaria, *Catal. Today*, 1997, **35**, 113.

11 M. A. Spronsen, J. W. M. Frenken and I. M. N. Groot, *Chem. Soc. Rev.*, 2017, **46**, 4347.

12 N. A. M. Barakat, M. H. El-Newehy, A. S. Yasin, Z. K. Ghouri and S. S. Al-Deyab, *Appl. Catal., A*, 2016, **510**, 180.

13 N. A. M. Barakat and M. Motlak, *Appl. Catal., B*, 2014, **154**, 221.

14 N. A. M. Barakat, M. Motlak, B. S. Kim, A. G. El-Deen, S. S. Al-Deyab and A. M. Hamza, *J. Mol. Catal. Chem.*, 2014, **394**, 177.

15 Z. K. Ghouri, N. A. M. Barakat and H. Y. Kim, *Sci. Rep.*, 2015, **5**, 16695.

16 Z. K. Ghouri, N. A. M. Barakat and H. Y. Kim, *Energy and Environment Focus*, 2015, **4**, 34.

17 B. Kaur, R. Srivastava and B. Satpati, *ACS Catal.*, 2016, **6**, 2654.

18 W. F. Simanullang, H. Itahara, N. Takahashi, S. Kosaka, K. Shimizu and S. Furukawa, *Chem. Commun.*, 2019, **55**, 13999.

19 A. Kubacka, M. Fernández-García and A. Martínez-Arias, *Appl. Catal., A*, 2016, **518**, 2.

20 R. J. M. Klein Gebbink and M.-E. Moret, *Non-Noble Metal Catalysis: Molecular Approaches and Reactions*, Wiley-VCH Verlag GmbH & Co. KGaA, 2019.

21 J. Gu, Y. W. Zhang and F. Tao, *Chem. Soc. Rev.*, 2012, **41**, 8050.

22 S. Cao, F. Tao, Y. Tang, Y. Lia and J. Yu, *Chem. Soc. Rev.*, 2016, **45**, 4747.

23 R. Glaser, *Nature*, 2015, **528**, 197.

24 S. J. Mejía-Rosales, C. Fernández-Navarro, E. Pérez-Tijerina, D. A. Blom, L. F. Allard and M. José-Yacamán, *J. Phys. Chem. C*, 2007, **111**, 1256.

25 L. Zhu, S. Shan, V. Petkov, W. Hu, A. Kroner, J. Zheng, C. Yu, N. Zhang, Y. Li, R. Luque, C. J. Zhong, H. Ye, Z. Yang and B. H. Chen, *J. Mater. Chem. A*, 2017, **5**, 7869.

26 L. Zhu, Y. Jiang, J. Zheng, N. Zhang, C. Yu, Y. Li, C. W. Pao, J. L. Chen, C. Jin, J. F. Lee, C. J. Zhong and B. H. Chen, *Small*, 2015, **11**, 4385.

27 L. Zhu, Z. Yang, J. Zheng, W. Hu, N. Zhang, Y. Li, C. J. Zhong, H. Ye and B. H. Chen, *J. Mater. Chem. A*, 2015, **3**, 11716.

28 J. F. Cahill, V. Kertesz and G. J. Van Berkel, *Anal. Chem.*, 2015, **87**(21), 11113.

29 Y. Suchorski, M. Datler, I. Bespalov, J. Zeininger, M. Stöger-Pollach, J. Bernardi, H. Grönbeck and G. Rupprechter, *Nat. Commun.*, 2018, **9**, 600.

30 J. Fan, H. Du, Y. Zhao, Q. Wang, Y. Liu, D. Li and J. Feng, *ACS Catal.*, 2020, **10**, 13560.

31 A. K. Rathi, M. B. Gawande, J. Pechousek, J. Tucek, C. Aparicio, M. Petr, O. Tomanec, R. Krikavova, Z. Travnicek, R. S. Varma and R. Zboril, *Green Chem.*, 2016, **18**, 2363.

32 I. S. Pieta, W. S. Epling, M. Garcıa-Dieguez, J. Y. Luo, M. A. Larrubia, M. C. Herrera and L. J. Alemany, *Catal. Today*, 2011, **55**, 175.

33 A. Goswami, A. K. Rathi, C. Aparicio, O. Tomanec, M. Petr, R. Pocklanova, M. B. Gawande, R. S. Varma and R. Zboril, *ACS Appl. Mater. Interfaces*, 2017, **9**, 2815.

34 T. Mazhar, V. Shrivastava, R. S. Tomar and J. Pharm, *Sci. Res.*, 2017, **9**, 102.

35 F. Tao, *Chem. Soc. Rev.*, 2012, **41**, 7977.

36 C. T. Campbell, *Annu. Rev. Phys. Chem.*, 1990, **41**, 775.

37 J. H. Sinfelt and J. A. Cusumano, *Bimetallic Catalysts: Discoveries, Concepts*; Wiley-Interscience: Hoboken, NJ, USA, 1983.

38 T. Jiang, Y. Zhou, S. Liang, H. Liu and B. Han, *Green Chem.*, 2009, **11**, 1000.

39 A. M. Molenbroek, J. K. Nørskov and B. S. Clausen, *J. Phys. Chem. B*, 2001, **105**, 5450.

40 F. Besenbacher, I. I. Chorkendorff, B. S. Clausen, B. Hammer, A. M. Molenbroek, J. K. Nørskov and I. I. Stensgaard, *Science*, 1998, **279**, 1913.

41 B. R. Cuenya, *Thin Solid Films*, 2010, **518**, 3127.

42 D. M. Alonso, S. G. Wettstein and J. A. Dumesic, *Chem. Soc. Rev.*, 2012, **41**, 8075.

43 N. E. Tsakoumis, A. P. E. York, D. Chena and M. Rønning, *Catal. Sci. Technol.*, 2015, **5**, 4859.

44 R. Cheula, M. Maestri and G. Mpourmpakis, *ACS Catal.*, 2020, **10**, 6149.

45 X. Liu, D. Wang and Y. Li, *Nano Today*, 2012, **7**, 448.

46 W. Zhang and X. Lu, *Nanotechnol. Rev.*, 2013, **2**, 487.

47 N. Tian, Z. Y. Zhou, S. G. Sun, Y. Ding and Z. L. Wang, *Science*, 2007, **316**, 732.

48 J. Wu, L. Qi, H. You, A. Gross, J. Li and H. Yang, *J. Am. Chem. Soc.*, 2012, **134**, 11880.

49 S. I. Choi, S. U. Lee, W. Y. Kim, R. Choi, K. Hong, K. M. Nam, S. W. Han and J. T. Park, *ACS Appl. Mater. Interfaces*, 2012, **4**, 6228.

50 J. W. Hong, D. Kim, Y. W. Lee, M. Kim, S. W. Kang and S. W. Han, *Angew. Chem., Int. Ed.*, 2011, **50**, 8876.

51 S. Iayoglu, A. Nilekar, M. Mavrikakis and B. Eichhorn, *Nat. Mater.*, 2008, **7**, 333.

52 G. Guisbiers, S. Khanal, F. Ruiz-Zepeda, J. Roque de la Puente and M. José-Yacaman, *Nanoscale*, 2014, **6**, 14630.

53 A. Nilekar, S. Alayoglu, B. Eichhorn and M. Mavrikakis, *J. Am. Chem. Soc.*, 2010, **132**, 7418.

54 F. Gao, Y. Cai, K. K. Gath, Y. Wang, M. S. Chen, Q. L. Guo and D. W. Goodman, *J. Phys. Chem. C*, 2009, **113**, 182.

55 J. Y. Park, Y. Zhang, M. Grass, T. Zhang and G. A. Somorjai, *Nano Lett.*, 2008, **8**, 673.

56 J. Y. Park, Y. J. Lee, P. R. Karandikar, K. W. Jun, K. S. Ha and H. G. Park, *Appl. Catal., A*, 2012, **411–412**, 15.

57 S. Dai, Y. You, S. Zhang, S. W. Cai, M. Xu, L. Xie, R. Wu, G. W. Graham and X. Pan, *Nat. Commun.*, 2017, **8**, 204.

58 M. Chi, C. Wang, Y. Lei, G. Wang, D. Li, K. L. More, A. Lupini, L. F. Allard, N. M. Markovic and V. R. Stamenkovic, *Nat. Commun.*, 2015, **6**, 8925.

59 https://phys.org/news/2015-11-ornl-microscopy-captures-real-time-view.html.

60 L. S. Kibis, D. A. Svintsitskiy, E. A. Derevyannikova, T. Yu. Kardash, E. M. Slavinskaya, O. A. Stonkus, V. A. Svetlichnyi and A. I. Boronin, *Appl. Surf. Sci.*, 2019, **493**, 1055.

61 J. Zhu, P. Xiao, H. Li and S. n. A. C. Carabineiro, *ACS Appl. Mater. Interfaces*, 2014, **6**, 16449.

62 Y. Wang, X. Wang and M. Antonietti, *Angew. Chem., Int. Ed.*, 2012, **51**, 68.

63 H. Xu, J. Yan, X. She, L. Xu, J. Xia, Y. Xu, Y. Song, L. Huang and H. Li, *Nanoscale*, 2014, **6**, 1406.

64 I. S. Pieta, A. Rathi, P. Pieta, R. Nowakowski, M. Hołdynski, M. Pisarek, A. Kaminska, M. B. Gawande and R. Zboril, *Appl. Catal., B*, 2019, **244**, 272.

65 P. Lakshmanan, *Micro and Nano Technologies*, 2019, **9**, 207.

66 Z. Zhao, Y. Suna and F. Dong, *Nanoscale*, 2015, **7**, 15.

67 Z. Sun, S. Wang, Q. Li, M. Lyu, T. Butburee, B. Luo, H. Wang, J. M. T. A. Fischer, C. Zhang, Z. Wu and L. Wang, *Adv. Sustainable Syst.*, 2017, **1**, 1700003.

68 S. Subhajyoti and S. Rajendra, *Energy Fuels*, 2017, **1**, 1390.

69 M. Tahir, N. Mahmood, J. Zhu, A. Mahmood, F. K. Butt, S. Rizwan, I. Aslam, M. Tanveer, F. Idrees, I. Shakir, C. Cao and Y. Hou, *Sci. Rep.*, 2015, **5**, 12389.

70 X. Li, A. F. Masters and T. Maschmeyer, *Chem. Commun.*, 2017, **53**, 7438.

71 Y. Gong, M. Li, H. Li and Y. Wang, *Green Chem.*, 2015, **17**, 715.

72 I. Agirrezabal-Telleria and E. Iglesia, *J. Catal.*, 2017, **352**, 505.

73 J. Xu, K. Shen, B. Xue and Y. X. Li, *J. Mol. Catal. Chem.*, 2013, **372**, 105.

74 T. S. Miller, A. Belen Jorge, T. M. Suter, A. Sella, F. Corà and P. F. McMillan, *Phys. Chem. Chem. Phys.*, 2017, **19**, 15613.

75 T. Sano, S. Tsutsui, K. Koike, T. Hirakawa, Y. Teramoto, N. Negishi and K. Takeuchi, *J. Mater. Chem. A*, 2013, **1**, 6489.

76 P. Praus, L. Svobod, M. Ritz, I. Troppová, M. Šihor and K. Kočí, *Mater. Chem. Phys.*, 2017, **193**, 438.

77 Ž. Petrović, M. Ristić, M. Marciuš, B. Sepiol, H. Peterlik, M. Ivanda and S. Musić, *Ceram. Int.*, 2015, **41**, 7811.

78 L. Wang, C. Wang, X. Hu, H. Xue and H. Pang, *Chem.–Asian J.*, 2016, **11**, 3305.

79 F. Dong, Z. Zhao, T. Xiong, Z. Ni, W. Zhang, Y. Sun and W. Ho, *ACS Appl. Mater. Interfaces*, 2013, **5**, 11392.

80 T. Jafari, E. Moharreri, A. S. Amin, R. Miao, W. Song and S. L. Suib, *Molecules*, 2016, **21**, 900.

81 Z. Zhao, Y. Sun and F. Dong, *Nanoscale*, 2015, **7**, 15.

82 Y. Che, Q. Liu, B. Lu, K. Wang and Z. Liu, *Sci. Rep.*, 2020, **10**, 721.

83 S. Naya, A. Inoue and H. Tada, *ChemPhysChem*, 2011, **12**, 2719.

84 X. Liu, D. Wang and Y. Li, *Nano Today*, 2012, **7**, 448.

85 B. Sneed, A. Young, D. Jalalpoor, M. Gloden, S. Mao and Y. Jiang, *ACS Nano*, 2014, **8**, 7239.

86 K. Vu, K. Bukhryakov, D. Anjum and V. Rodionov, *ACS Catal.*, 2015, **5**, 2529.

87 Y. Di, X. Wang, A. Thomas and M. Antonietti, *ChemCatChem*, 2010, **2**, 834.

88 C. Han, Y. Lu, J. Zhang, L. Ge, Y. Li, C. Chen, Y. Xin, L. Wu and S. Fang, *J. Mater. Chem. A*, 2015, **3**, 23274.

89 K. Maeda, *Phys. Chem. Chem. Phys.*, 2013, **15**, 10537.

90 C. Ding, C. Feng, Y. Ji, F. Liu, H. Wang, M. Dupuis and C. Li, *Appl. Catal., B*, 2020, **268**, 118391.

91 J. Xue, S. Ma, Y. Zhou, Z. Zhang and M. He, *ACS Appl. Mater. Interfaces*, 2015, **7**, 9630.

92 C. Han, L. Wu, L. Ge, Y. Li and Z. Zhao, *Carbon*, 2015, **92**, 31.

93 H. Jiang, S. Gong, S. Xu, P. Shi, J. Fan, V. Cecen, Q. J. Xu and Y. L. Min, *Dalton Trans.*, 2020, **49**, 5074.

94 A. Vasileff, C. Xu, Y. Jiao, Y. Zheng and S. Z. Qiao, *J. Am. Chem. Soc.*, 2019, **141**, 2490.

95 D. Y. Chung, K. J. Lee and Y. E. Sung, *J. Phys. Chem. C*, 2016, **120**, 9028.

96 G. Long, X. Li, K. Wan, Z. Liang, J. Piao and P. Tsiakaras, *Appl. Catal., B*, 2017, **203**, 541.

97 N. A. M. Barakat, M. Motlak, B. H. Lim, M. H. El-Newehy and S. S. Al-Deyab, *J. Electrochem. Soc.*, 2014, **161**, F1194.

98 P. J. Kulesza, I. S. Pieta, I. A. Rutkowska, A. Wadas, D. Marks, K. Klak, L. Stobinski and J. A. Cox, *Electrochim. Acta*, 2013, **110**, 474.

99 W. Huang, H. Wang, J. Zhou, J. Wang, P. N. Duchesne, D. Muir, P. Zhang, N. Han, F. Zhao, M. Zeng, J. Zhong, C. Jin, Y. Li, S. T. Lee and H. Dai, *Nat. Commun.*, 2015, **6**, 10035.

100 K. Vu, K. Bukhryakov, D. Anjum and V. Rodionov, *ACS Catal.*, 2015, **5**, 2529.

101 L. Liu, E. Pippel, R. Scholz and U. Gçsel, *Nano Lett.*, 2009, **9**, 4352.

102 H. Qian, S. Chen, Y. Fu and X. Wang, *J. Power Sources*, 2015, **300**, 41.

103 A. Lewalska-Graczyk, P. Pieta, G. Garbarino, G. Busca, M. Holdynski, G. Kalisz, A. Sroka-Bartnicka, R. Nowakowski, M. Naushad, M. B. Gawande, R. Zbořil and I. S. Pieta, *ACS Sustainable Chem. Eng.*, 2020, **8**, 7244.

104 X. Wang, M. Sun, Y. Guo, J. Hu and M. Zhu, *J. Colloid Interface Sci.*, 2020, **558**, 38.